

X-ray Photoelectron Spectroscopy analysis and characterization of $\text{Gd}_2\text{O}_2\text{S:Tb}^{3+}$ phosphor powder

J.J. Dolo*, F.B. Dejene, J.J Terblans, O.M. Ntwaeaborwa and H.C. Swart*

Physics Department, University of the Free State, P.O. Box 339, Bloemfontein, 9300, South Africa

*Corresponding author: dolojj@qwa.ufs.ac.za or SwartHC@ufs.ac.za

Abstract. This paper presents the X-ray Photoelectron Spectroscopy (XPS) analyses of the electron beam degraded and undegraded $\text{Gd}_2\text{O}_2\text{S:Tb}^{3+}$ phosphor powder. The XPS data was collected from $\text{Gd}_2\text{O}_2\text{S:Tb}^{3+}$ phosphor powders before and after electron beam degradation. The data confirms the presence of Gd_2O_3 and Gd_2S_3 from both the degraded and undegraded powders. In addition, S-O bonding was also detected from degraded powders. This clearly indicates that the surface reaction did occur during prolonged electron bombardment in an oxygen atmosphere.

1. Introduction

Terbium doped gadolinium oxysulfide ($\text{Gd}_2\text{O}_2\text{S:Tb}^{3+}$), one of the rare earth oxysulfide group of phosphors, is known to be an efficient phosphor and has been put to practical application in low voltage cathodoluminescent and X-ray devices because of its high conversion efficiency (12–25%) of the exciting radiation [1-3]. $\text{Gd}_2\text{O}_2\text{S:Tb}^{3+}$ is a well-known green-emitting photoluminescence and cathodoluminescence phosphor used in high resolution and projection television screens [4-7]. We report the XPS characterization of commercial terbium doped gadolinium oxysulfide ($\text{Gd}_2\text{O}_2\text{S:Tb}^{3+}$) green phosphor, which was evaluated for possible application in cathode ray tube CRT and field emission display (FED) screens.

2. Characterization

Auger electron spectroscopy (AES) and Cathodoluminescence (CL) spectroscopy were used respectively to monitor changes on the surface and the CL properties. The AES measurements were taken in an UHV chamber using a PHI model 549 Auger spectrometer. The chamber was first evacuated to 2.8×10^{-9} Torr before backfilling with oxygen to 1×10^{-6} Torr. Scanning Electron Microscopy (SEM) images were taken with a Gemini LEO 1525 Model to determine the particle morphology. The crystalline structure of the phosphor powders were investigated using a Burker D8 (Burker Co, German) X-ray diffractometer with $\text{Cu K}\alpha = 1.5406 \text{ \AA}$. The $100 \mu\text{m}$, 25 W, 15 kV energy X-ray beam was used to analyze the S 2p, O 1s, Gd 3d and Gd 4d binding energy peaks (pass energy 11.8 eV, analyser resolution ≤ 0.5 eV). The possible chemical states were identified with the Multipak version of 8.2c computer software [8] using Gaussian-Lorentz fits.

3. Results and Discussion

Figure 1 shows the XRD pattern of the $\text{Gd}_2\text{O}_2\text{S}:\text{Tb}^{3+}$ phosphor powder. The position and relative intensity of the XRD lines are in good agreement with the data of JSPDS file No.26-1422, which shows the pure $\text{Gd}_2\text{O}_2\text{S}$ hexagonal structure.

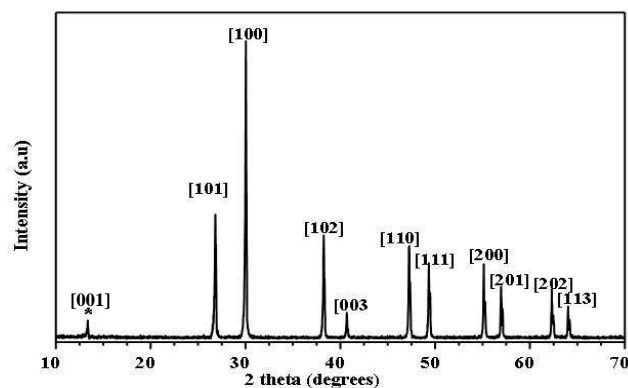


Figure 1: XRD pattern for the $\text{Gd}_2\text{O}_2\text{S}:\text{Tb}^{3+}$ phosphor powder.

Figure 2 (a) shows the SEM image of the $\text{Gd}_2\text{O}_2\text{S}:\text{Tb}^{3+}$ phosphor powder. The particles are polyhedron in shape and agglomerated, showing relatively good close packing which is one requirement for the CRT or X-ray intensifying screens and the particles differ in sizes and shapes. EDS data in figure 2 (b) confirms the presence of all the elements (Gd, O and S) together with the adventitious carbon. Tb^{3+} ions were not detected probably due to their relatively low concentration in the $\text{Gd}_2\text{O}_2\text{S}:\text{Tb}^{3+}$ matrix.

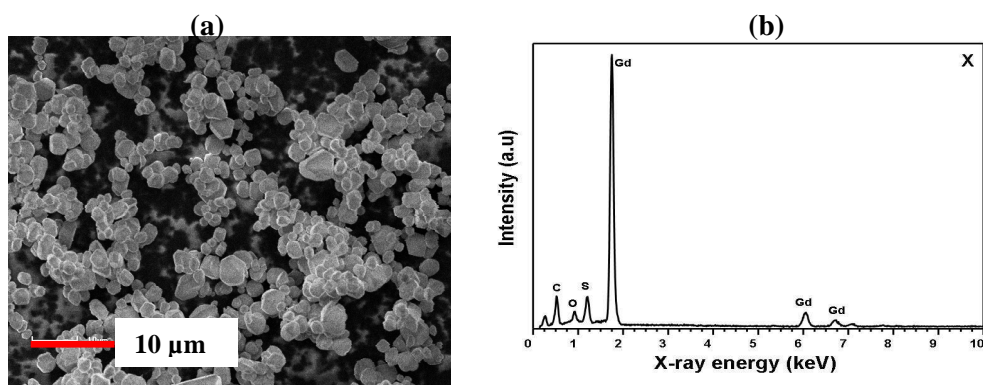


Figure 2: (a) SEM image and (b) EDS spectra marked X of the $\text{Gd}_2\text{O}_2\text{S}:\text{Tb}^{3+}$ phosphor powder.

Figure 3 (a) shows the CL spectra before degradation and after degradation as function of wavelength. The CL decreased due to the formation of a new non-luminescent surface oxide layer. The main emission peak due to the $^5\text{D}_4 \rightarrow ^7\text{F}_5$ transition is at a wavelength of 545 nm. Less intense emission peaks at 490 nm, 585 nm and 620 nm due to the $^5\text{D}_4 \rightarrow ^7\text{F}_j$ ($J = 0, 1, 2, 3, \dots$) transitions are also shown. The main emission peak at 545 nm was only about 45% of the initial intensity after degradation. Figure 3 (b) shows the PL spectra of $\text{Gd}_2\text{O}_2\text{S}:\text{Tb}^{3+}$ powder phosphors excited at 254 nm. The luminescence peaks in the figure arise from the transitions of the $^5\text{D}_4$ excited state levels to $^7\text{F}_j$ ($J = 0, 1, 2, 3, 4, \dots$) ground state levels, and belong to the characteristic emission of Tb^{3+} . The emission line at 490 nm corresponds to the $^5\text{D}_3 \rightarrow ^7\text{F}_6$ transitions, and the emission lines between the 585 and 620

nm corresponds to the $^5D_4 \rightarrow ^7F_4$ and $^5D_4 \rightarrow ^7F_3$ transitions respectively. The peak at 545 nm arising from the $^5D_4 \rightarrow ^7F_3$ transition has the highest intensity.

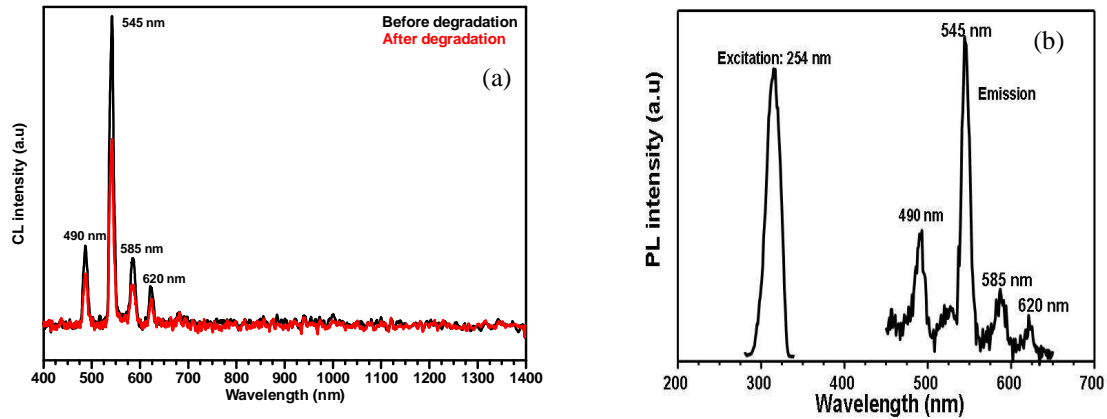


Figure 3: (a) CL before and after degradation 1×10^{-6} Torr and (b) PL spectra for $Gd_2O_2S:Tb^{3+}$ phosphor powder.

Figure 4 shows fitted high resolution S 2p XPS spectra (a) before and (b) after degradation at 1×10^{-6} Torr O_2 . Note that it is well known that the S 2p consists of $2p_{3/2}$ (BE = ~ 163 eV) and $2p_{1/2}$ (BE = ~ 165 eV) peaks. XPS spectrum in figure 4 (a) indicates that sulfur was primarily present as Gd_2O_2S (BE = ~ 165 eV) plus a small amount of sulfide species (BE = ~ 158 eV). The peak at BE = ~ 158 eV can be assigned to Gd_2S_3 [9]. In addition, the fitted data shows an evidence of oxides species (SO_2) at BE = ~ 168 eV. The degraded spectrum in figure 4 (b) shows an increase in the Gd_2S_3 and SO_2 peak intensity suggesting that an electron beam induced surface chemical reaction occurred between S and Gd, and S and O.

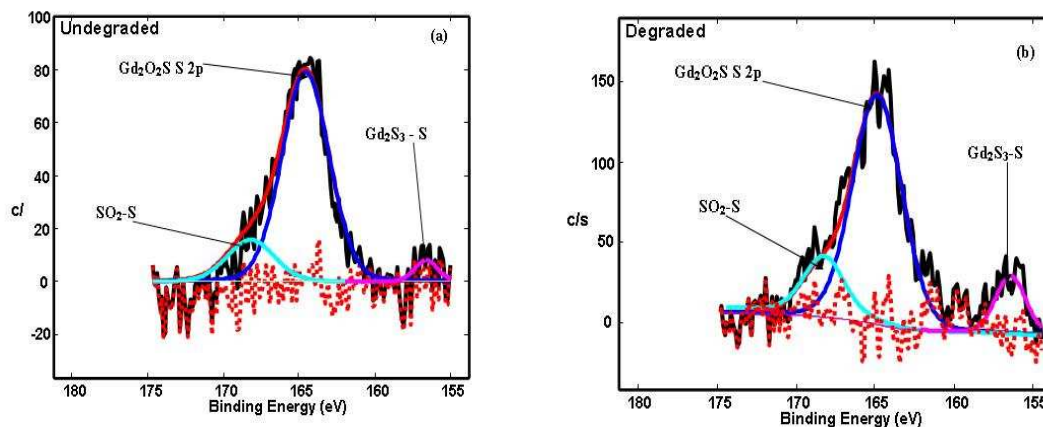


Figure 4: Fitted XPS for S 2p of $Gd_2O_2S:Tb^{3+}$ phosphor powder peaks (a) before and (b) after degradation for 1×10^{-6} Torr.

Figure 5 shows fitted XPS for O1s peaks (a) before and (b) after degradation for 1×10^{-6} Torr obtained at O 1s at 531.3 eV. It can be noted that both the degraded and undegraded powder spots only two binding energy peaks were identified. The Gd_2O_3 peak however shows an increase in intensity for the degraded sample. The growth in Gd_2O_3 after degradation is due to the oxide formation on the surface as a result of the ESSCR process as observed in the APPH results [9]. It is therefore clear that a

chemical reaction occurred during the degradation process. The binding energy assignment of the mixed oxides is based on a large extent to the core level screening that occurs in O^{2-} anion compared to the other oxygen species that are present on the surface and the relative magnitude of this peak compared to other O 1s peaks present [10].

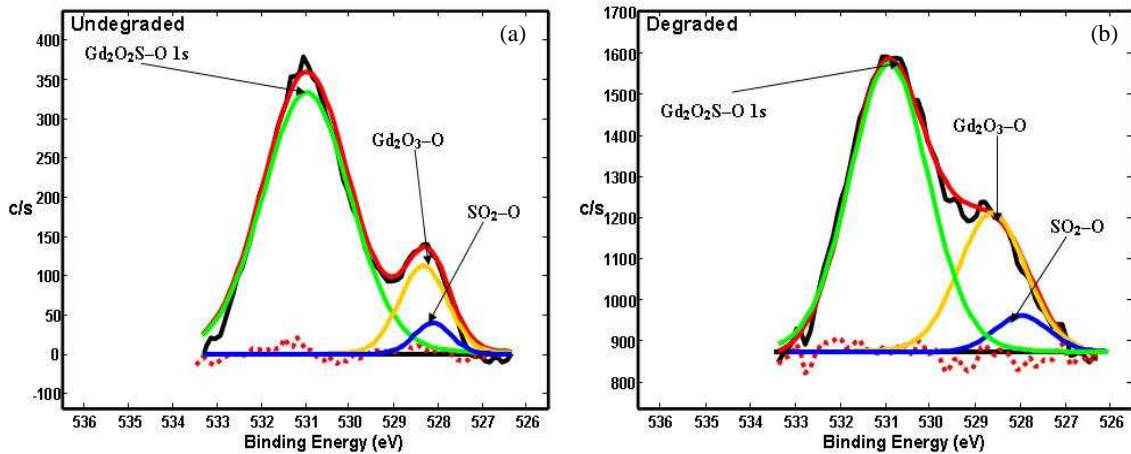


Figure 5: Fitted XPS for O 1s of $Gd_2O_2S:Tb^{3+}$ phosphor powder peaks (a) before and (b) after degradation for 1×10^{-6} Torr.

Figure 6 shows the fitted results from an XPS spectrum of the Gd 3d peaks (a) before and (b) after degradation. The peak shape changed due to an extra peaks of Gd_2O_3 (1189.0 eV) and Gd_2S_3 (1192.2 eV) that developed at higher binding energies. Gd_2O_2S -Gd 3d peaks were measured at 1185.20 eV. Both the degraded powder and undegraded spots recorded one peak of Gd_2O_2S -Gd 3d. The peaks for Gd_2O_3 and Gd_2S_3 after degradation have grown and this clearly shows that the surface reaction did occur after degradation.

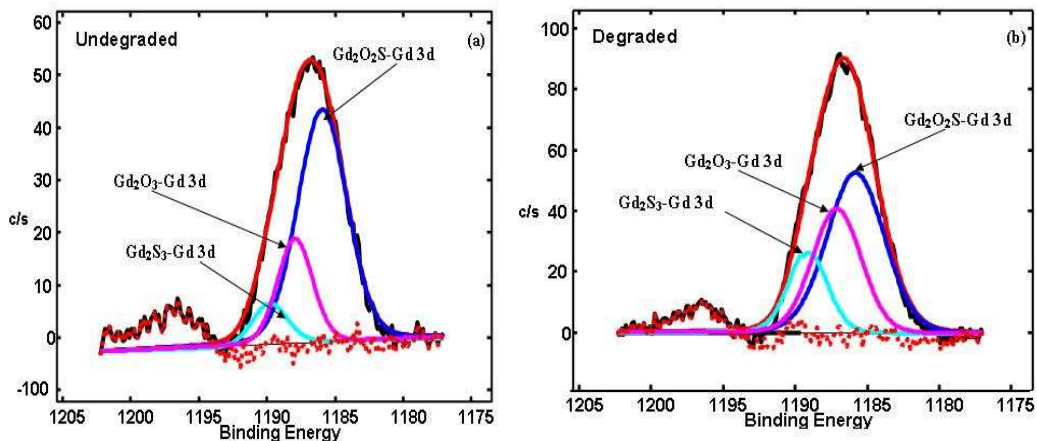


Figure 6: Fitted XPS for Gd 3d of $Gd_2O_2S:Tb^{3+}$ phosphor powder peaks (a) before and (b) after degradation for 1×10^{-6} Torr.

Figure 7 shows the Gd 4d peaks position for the Gd_2O_2S (Gd_2O_2S -4d peaks) (a) before and (b) after degradations. Six peaks can be identified for the Gd 4d core level spectrum after deconvolution of the experimentally measured curve. Gd $4d_{3/2}$ and Gd $4d_{5/2}$ peaks of the Gd_2O_2S are located at 146.7 eV and

141.6 eV. In addition, there are two peaks measured at 142.2 eV and 147.3 eV that can be associated with Gd_2O_3 and the small peaks measured at 147.9 eV and 144.8 eV that can be associated with Gd_2S_3 . There is also an increase in relative ratio of the peaks, this suggests that a surface chemical reaction occurred and another possibility for the presence of the peaks (Gd_2O_3 and Gd_2S_3) could be chemical decomposition of the material [11].

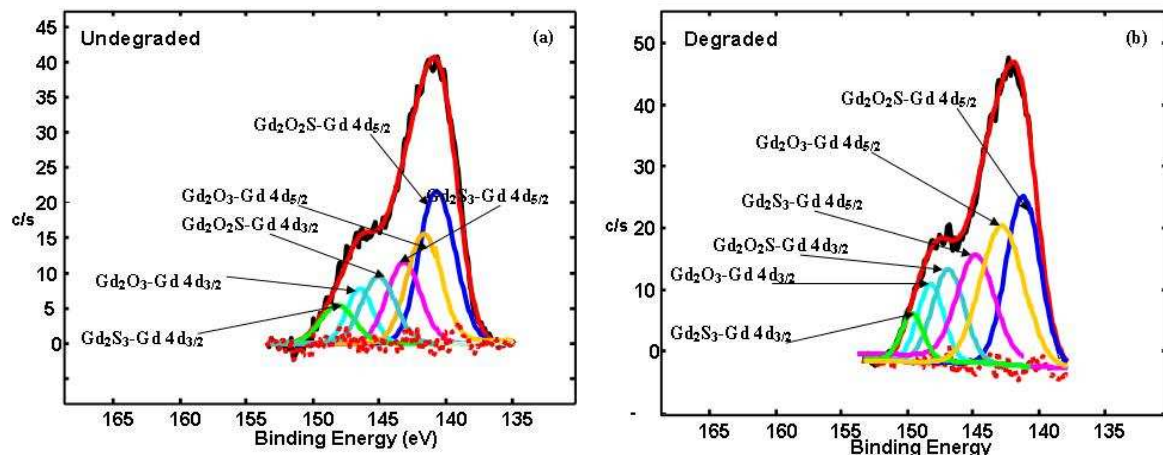


Figure 7: Fitted XPS for Gd 4d of $Gd_2O_2S:Tb^{3+}$ phosphor powder peaks (a) before and (b) after degradation for 1×10^{-6} Torr.

4. Conclusion

The XPS results confirmed the presence of Gd_2O_3 and Gd_2S_3 on the degraded $Gd_2O_2S:Tb^{3+}$ powder spots. The XRD pattern of $Gd_2O_2S:Tb^{3+}$ powder shows hexagonal phase structure. The EDS confirms the presence of all elements of the host matrix (Gd_2O_2S) as well as the adventitious carbon from the surface. The PL properties were also investigated.

Acknowledgement

The authors send gratitude to the National Research Foundation (NRF) for funding the project and the University of Free State (Physics department, Center for microscopy and Geology department) for the research techniques used in this study.

Reference

- [1] Royce MR, 1968 US Patent 3 **418** 246
- [2] Royce MR, Smith AL, 1968 Electrochem. Soc., Spring Meeting Extended Abstracts, **34** 94
- [3] Giakoumakis GE, Pallis A, 1989 J., Solid State Comm. **70** 419
- [4] Blasse G, Grabmaier BC, 1994 Luminescence Material, Springer-Verlag, New York
- [5] Popovici EJP, Muresan L, Hristea-Simoc A, Indrea E, Vasilescu M, Nazarov M, Jeon DY, 2002 Opt. Mat., **29** 632
- [6] Jiang Y, Wu Y, 2000 J. Am. Ceram. Soc., **83** 2628
- [7] Yamamoto H, Kano T, 1979 J. Electrochem. Soc., **126** 305
- [8] Moulder F, Stickle WF, Sobol PE, Bombardier KD, 1995 Handbook of X-ray Photoelectron Spectroscopy, ULVAC-PHI, Inc., 370 Enzo, Chigasaki, **143** Japan
- [9] Dolo JJ, Swart HC, Coetsee E, Terblans JJ, Ntwaaborwa OM and Dejene BF, 2010 Hyperfine Inter., **197** 129
- [10] Hashimoto AK, X-ray photoelectron spectra of several oxides, **1977** Corros. Sci., 17 559
- [11] Datta P Majewski, F Aldinger, 2009 Mat. Charac., **60** 138